

Single Walled Boron Nitride Nanotube Reinforced Composite Based Nanomechanical Resonator

Prabhat Kumar Tripathi(1)
M.Tech. student, Noise & vib.
control lab MIED, IIT
Roorkee, 247667

S. P. Harsha(2)
Assoc. Prof. Noise & vib.
control lab MIED, IIT,
Roorkee, 247667

S. H. Upadhyay(3)
Asst. Prof. Noise & vib. control
lab MIED, IIT
Roorkee, 247667

“Abstract”

The suitability of the Boron Nitride Nanotubes (BNNTs) reinforced polymeric composites as nanomechanical resonators, using continuum mechanics approach and finite element method (FEM) is illustrated in this paper. Continuum mechanics based approach using analytical formulation is used to examine the mass sensitivity of single walled BNNT (SWBNNT) reinforced composite for varying aspect ratios and volume fractions of SWBNNT in composites. SWBNNT is considered as a transversely anisotropic material, finite analysis is performed and results are compared with the analytical approach. The results indicated that the mass sensitivity of SWBNNT reinforced composite based nanomechanical resonators can reach $10^{-3}fg$ ($10^{-21}Kg$) and a logarithmically linear relationship exist between the resonant frequency and the attached mass, when mass is larger than $10^{-3}fg$. The simulation results based on present FEM found are in good agreement with the analytical approach used in this paper.

“1. Introduction”

Due to the remarkable properties in many aspects, for example, the chirality and diameter-independent semi-conductivity[1-3], the excellent thermal conductivity[3-5], the high elastic modulus[6,7] and the high resistance to oxidation[3,8,9], boron nitride nanotubes (BNNTs) are expected to be attractive candidates for promising applications in composite materials and nanoscale electrical devices working under extreme conditions. However, the limited dispersion of BNNTs in conventional solvents and the poor interfacial interaction with the polymer matrix hinder their applications. In the last few years, many efforts have been devoted to the surface modification towards their dispersibility and surface adhesion improvement [10]. Boron nitride nanotubes (BNNTs), which are

structurally similar to CNTs, have been predicted to behave like wideband-gap semiconductors independent of radius, chirality, and the number of tubular shells[1]. Moreover, BNNTs have superb mechanical properties, thermal conductivity, and resistance to oxidation at high temperatures [11]. These factors may promote effective BNNT usage in nano composites. However, studies of BNNTs–polymer composites are almost absent, because it is extremely difficult to obtain a highly pure BNNT phase with a yield high enough to fabricate and test a composite material, although many methods have been probed to synthesize BNNTs [11]. BNNTs are, therefore, more suitable for reinforcement of composite materials for applications especially at elevated temperatures in oxidizing environment.

A number of studies are currently available on metal, ceramic and polymer matrix composites reinforced with CNTs as seen from the recent review articles. However, until now, not many results have been published on the subject of BNNTs reinforced composites. The objective of this work was to analyse the dynamic behaviour of BNNT reinforced composite based mass sensor to improve the strength and fracture toughness of a polymer by reinforcing with BN nanotubes. Resonance frequencies of polymer-BN nanotube composite were determined by attaching varying mass at different locations of composite for cantilevered boundary conditions. Publications of BNNTs have not been explored as vastly as CNTs. With increasing interest in BNNT and its composites, several potential applications are being proposed. Carbon doped BNNTs are suitable for field emitters with better environmental stability [3]. Polymer based nano composites containing BNNTs offer wide range applications in optoelectronics, light-harvesting, and related phenomena. In addition, BNNTs manifest improved thermal properties and were used as insulating composites of high thermal conductivity as in BNNTs; the thermal transfer mainly takes place via the phonons, not electrons [12]. BNNTs possess piezoelectric characteristics which could be used in

precision piezoelectric devices to measure or apply force at high resolution [13]. BNNT also has bright prospects for non-linear optical and optoelectronic applications. BNNTs may be ideal candidates for optical devices working in the UV regime [14]. Gas adsorption ability of BNNT may also be used for hydrogen storage and thus offering solution to current environmental pollution [15]. Apart from the above listed applications, BNNT is gaining popularity as reinforcement in polymer and ceramic matrix composites due to its excellent mechanical and thermal properties.

Resonance-based sensors offer the potential of meeting the high performance requirement of many sensing applications including metal deposition monitors, chemical reaction monitors, biomedical sensors, mass detectors, etc. These types of sensors work on the characteristic in frequency shift due to mass loading. The micromechanical resonators, such as micro cantilevers, have received much attention in recent years [17]. The merit of micromechanical resonators is that miniaturization of their dimensions enhance the mass sensitivity of these sensors. It has been reported that the detectable mass can be as small as several femtograms by using micro-sized silicon or silicon nitride cantilevers [18, 19]. It is now accepted that nanotechnology may considerably enhance strength/damping behaviour and reduce noise of engineering structures through the utilisation of nanomaterials that dissipate a substantial fraction of the vibration energy that they receive [20]. Several literatures are found addressing the issues related to resonant frequency based mass detection using nanomechanical resonators with different issues raised during adsorption of the molecules to the surface of the nanomechanical resonators. Arlett et al. [21] reported micro- and nanoscale biosensors specially cantilevered configuration of surface-stress and dynamic mode mechanical biosensors with particular focus on fast mechanical biosensing in fluid by mass- and force-based methods and challenges by nonspecific interaction. Eom et al. [22] reported the issues of special relevance to the dynamic behaviour of micro-or nanoresonators and their applications in biological or chemical detections and physical models of various nanoresonators such as nanowires, carbon nanotubes and graphene were discussed to design resonator-based applications for special purpose such as single molecular detection.

Chopra and Zettl, [6] reported mechanical measurement of BNNTs, where the amplitude of thermally-induced vibration of a cantilevered BNNT was examined at room temperature inside *transmission electron microscopy (TEM)* and the elastic modulus of a single

BNNT was estimated to be 1.22-0.24 TPa. Ciofani et al. [23] exploited the use of BNNTs in the nanomedicine field and reported that BNNTs are more suitable for the development of sensors and transducers for the detection of biological entities, due to their chemical stability. In the present study, to find out the mass sensitivity limit of BNNT reinforced polymeric composite and its suitability as a mass detector for many mass sensing applications, different masses were attached at three different positions i.e. at the end, at the middle and at one-third position from fixed end of cantilever configuration and analysed.

The resonant frequency of a BNNT reinforced composite for cantilevered (cantilevered) boundary condition with attached mass varying from 10^{-3} fg to 1 fg is analyzed. SWBNNT is taken as a thin walled tube of outer diameter 1.34nm and thickness of 0.34nm, for different aspect ratios as well as for different volume fractions of BNNT in composite. FEM simulation results are compared with analytical approach and are found in good agreement with later for its suitability for analysis of wide range of applications of BNNTs based composites.

“2. Vibration Analysis of SWBNNT Reinforced Composite”

The continuum models based on beam as well as shell have been used extensively for carbon nanotubes (CNTs) [24-26]. This motivates to use the continuum model of BNNT reinforced composite, for obtaining analytical expressions to relate the resonant frequency of attached mass using a rod based on the Euler Bernoulli beam theory [27]. The equation of motion of free vibration can be expressed as:

$$EI \frac{\partial^2 y}{\partial x^2} + \rho A \frac{\partial^2 y}{\partial t^2} = 0 \quad (1)$$

Where, E is Young's modulus, I is the second moment of the cross-sectional area A, and ρ is the density of the material. Depending on the boundary condition of the BNNT reinforced composite and the location of the attached mass, the resonant frequency of the combined system can be derived.

The fundamental resonant frequency can be expressed as:

$$f_n = \frac{1}{2\pi} \sqrt{\left(\frac{K_{eq}}{m_{eq}}\right)} \quad (2)$$

Where, k_{eq} and m_{eq} are equivalent stiffness and equivalent mass of BNNT reinforced composite with attached mass. The end condition namely, cantilevered

is being considered in this paper. The additional mass is assumed to be attached at the free end, at the middle and at one third position of cantilevered beam.

“2.1 SWBNNT reinforced composite with attached mass at different positions from fixed end for cantilevered configuration”

Fig.1 shows cantilevered configuration of SWBNNT reinforced composite nanomechanical resonator, in this case considering added mass M giving a virtual force at the location of the mass so that the deflection under the mass becomes unity. For this case harmonic motion and kinetic energy of single walled BNNT composite, equivalent stiffness (K_{eq}), velocity along the length of single walled BNNT composite, K.E. of the constraint and equivalent mass (m_{eq}) can be obtained as :-

$$\text{Equivalent stiffness, } K_{eq} = \frac{3E_{av}l}{l} \tag{3}$$

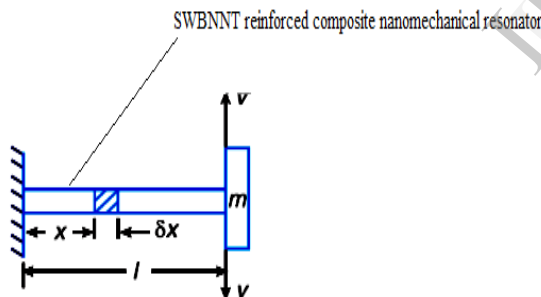
Consider a constraint whose one end is fixed and the other end is free as shown in Fig. 1.

Consider the cantilever with mass M at different positions from the fixed end.

Let M_1 = Mass of beam per unit length; l = length of beam

$$M_b = M_1 \cdot l = \rho_{eq} \cdot A_{eq} \cdot l = \text{total mass of cantilever.}$$

The inertia factor due to mass of beam = $\left(\frac{33}{140} M_b\right)$



“Fig. 1 Effect of inertia of the constraint in transverse vibrations.”

v = Transverse velocity of the free end

Consider a small element of the constraint at a distance x from the fixed end and of length δx , the velocity of this element is given by: The velocity of small element is given by:

$$dv = \frac{3 \cdot l \cdot x^2 - x^3}{2 \cdot l^3} v \tag{4}$$

Kinetic energy of the element thus can be obtained as:

$$\Delta KE = \frac{1}{2} \cdot M_1 \cdot \delta x \cdot \left[\left(\frac{3 \cdot l \cdot x^2 - x^3}{2 \cdot l^3} v \right)^2 \right] \tag{5}$$

Therefore the total kinetic energy of the system is obtained by integrating above equation

$$KE = \int_0^l \Delta KE \tag{6}$$

$$KE = \frac{M_1 \cdot v^2}{8 \cdot l^6} \int_0^l (9 \cdot l^2 \cdot x^4 - 6 \cdot l \cdot x^5 + x^6) \cdot dx \tag{7}$$

$$= \frac{M_1}{8 \cdot l^6} v^2 \left(\frac{33}{35} l^7 \right) = \frac{1}{2} \left[\left(\frac{33}{140} M_b \right) v^2 \right] \tag{8}$$

If a mass of $\left(\frac{33}{140} M_b\right)$ is placed at the free end and the constraint is assumed to be of negligible mass, then

$$\text{Total kinetic energy possessed by the constraint} = \frac{1}{2} \left[\left(\frac{33}{140} M_b \right) v^2 \right] \tag{9}$$

Hence, the two systems as represented by equations (8) and (9) are dynamically same. Therefore, the inertia of the constraint may be allowed for by adding $\frac{33}{140}$ of its mass to the beam at the free end.

Voigt upper bound and Reuss lower bound model (V-R model) [28] is used in this paper for calculating the average Young’s modulus of composite. For this it is assumed that aligned fibres (BNNTs), and fibres and matrix are subjected to the same uniform strain in the fibre direction, Voigt got the effective modulus in the fibre direction (E_{eq}) as:

$$E_{eq} = E_t V_t + E_m (1 - V_t) \tag{10}$$

Where, E_t and E_m are Young’s modulus for BNNT and matrix (PMMA) material respectively.

Reuss applied the same uniform stress on the fibre and matrix in the transverse direction, and got the effective modulus in the transverse direction

$$(E_{eqt}) \text{ as:}$$

$$\frac{1}{E_{eqt}} = \frac{V_t}{E_t} + \frac{V_m}{E_m} = \frac{V_t}{E_t} + \frac{(1-V_t)}{E_m} \tag{11}$$

Where, V_t is the volume fraction of fibre in the two-phase composite system, and subscripts “t” and “m” respectively refers to the fibre (tube) and matrix material. Equation (10) is the parallel coupling formula, and it is also called the “rule of mixtures”, whereas (11) is the series coupling formula, and it is also called the “inverse rule of mixtures”.

The volume fraction of BNNT in composite can be obtained by using the relation:

$$V_t = \frac{n \cdot \pi (r_o^2 - r_i^2)}{3\sqrt{2} a^2 - n \cdot \pi \cdot r_i^2} \tag{12}$$

Where, n=no. of BNNTs in composite

r_o and r_i = outer and inner radius of BNNT
 a = side of hexagonal RVE

For calculating average young’s modulus of composite (E_{av}), it is assumed that:

$$E_{av} = \frac{E_{eq} + 2E_{eqt}}{3} \tag{13}$$

Equivalent density (ρ_{eq})

$$\rho_{eq} = \rho_t Vt + \rho_m(1 - Vt) \quad (14)$$

Where, ρ_t and ρ_m are mass density of tube and matrix materials respectively.

For mass less cantilever and a load of M attached at distance of 'a' from the fixed end, the frequency can be obtained as:

$$f_{n1} = \frac{1}{2\pi} \sqrt{\left(\frac{2.E.I}{M.a^2(l-\frac{a}{3})}\right)} = \frac{1}{2\pi} \sqrt{A} \quad (15)$$

And the natural frequency for a massed cantilever is;

$$f_{n2} = \frac{1}{2\pi} \sqrt{\left(\frac{3.E.I}{\left(\frac{33}{140}\rho_{eq}.A_{eq}.l\right)l^3}\right)} = \frac{1}{2\pi} \sqrt{\left(\frac{140.E.I}{11.\rho_c.A_c.L_c^4}\right)} = \frac{1}{2\pi} \sqrt{B} \quad (16)$$

Natural frequency for mass attached at distance of 'a' from fixed end can be obtained by using Dunkerley's Empirical formula as:

$$\frac{1}{f_n^2} = \frac{1}{f_{n1}^2} + \frac{1}{f_{n2}^2} \quad (17)$$

$$\frac{1}{(f_n)^2} = \frac{4.\pi^2}{A} + \frac{4.\pi^2}{B} = 4.\pi^2(K_1 + K_2) \quad (18)$$

Where $K_1 = \frac{1}{A}$ and $K_2 = \frac{1}{B}$,

$$f_n = \frac{1}{2.\pi.\sqrt{(K_1+K_2)}} \quad (19)$$

“3. Modelling and Analysis of Boron Nitride nanotube reinforced Composite.”

With the emerging field of nanotechnology, there seems a greater need than ever to be able to carry out computational simulations. This is because the material and devices related to the nanotechnology are often on the atomic scale and thus extremely difficult and costly to fabricate & manipulate. With the increasing computational power over the past few years and improvements in theoretical methods and algorithms and finite element techniques, the capability of simulation has greatly expanded. In this paper, continuum mechanics approach has also been used.

“3.1 Continuum Mechanics (CM) Approach”

In spite of the constant increase in the last several years in computational speed, storage availability and improvement in numerical algorithms, MD computations are still limited to simulations of the order of 10^6 atoms for only a few nanoseconds [29]. The simulation of larger systems or longer times can only be achieved by other methods, typically, continuum methods. In continuum methods, however,

mechanical simulation methods completely discard variations over lengths on the order of the atomic scale as well as the atomic structure of the CNTs. Several advanced methods were developed towards continuum simulations and were applied to CNTs. Some of these methods are reviewed in [29] and include the quasi-continuum method [30-31], which incorporates interatomic interactions into an adaptively refined finite elements model through a crystal calculation, and the equivalent-continuum model [32], in which a representative volume element of the chemical structure of graphene was substituted with equivalent-truss and equivalent-continuum models. The basic continuum shell model was also shown to describe the mechanics of CNT accurately when proper parameters are chosen [34]. Finite elements (FE) analysis packages, such as ABAQUS were implemented to produce results which are very similar to experimental observations, such as the rippling of nanotubes at large deformations [33]. The similar concept is applied here for modelling and simulation of BNNT reinforced composites.

In this paper, BNNT reinforced composites has been modelled using SOLIDWORKS. The hexagonal RVE and long BNNT inside the RVE has been taken with following parameters;

Side of hexagonal RVE = 6.5 nm, Aspect ratio (L/D) = 500 and 100, No. of tubes = 5 and 10, Outer diameter of tube = 1.34 nm, Inner diameter of tube = 0.66 nm.

Models of BNNT reinforced composites are analysed using FEM based technique with ABAQUS software. The different parameters used in the analysis of composite are described in table (1).

“Table 1:- Parameters taken for analysis.”

Properties	For matrix material	For BNNT
Density	1.18 gm/cm ³	2.28 gm/cm ³
Young's modulus	3 GPa (For PMMA)	1180 GPa
Poisson's ratio	0.35	0.25

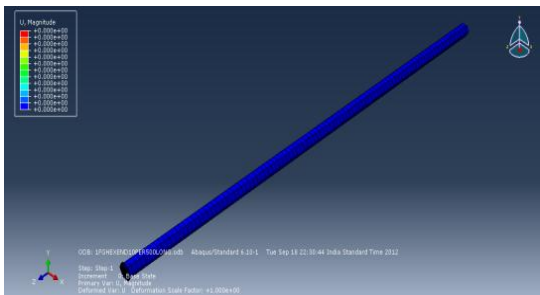
For mass sensitivity analysis, the different values of mass varying from 1 fg to 10^{-3} fg are attached at various positions of composite for cantilevered boundary condition.

“4. Result and discussion”

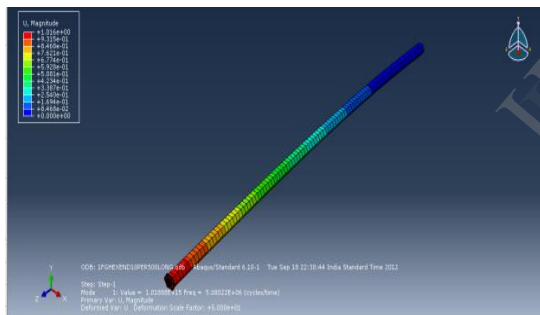
Continuum mechanics based analysis is carried out by considering BNNTs as a thin shell having outer diameter 1.34 nm and thickness of 0.066 nm. The other conditions like different L/D ratios (100 and 500) and

varying volume fractions of BNNT in composite (6% and 12%) have also been taken for analysis.

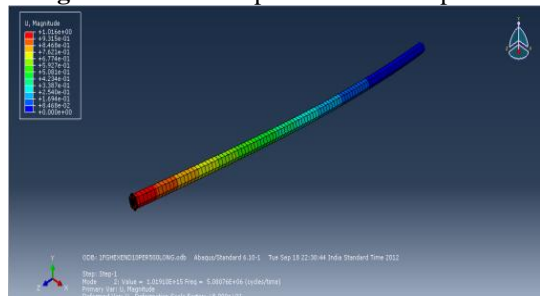
In the present study, the resonant frequencies of the cantilevered BNNT reinforced composites due to varying mass attached at the end, centre and one third position are analysed. The Euler–Bernoulli theory with cantilevered boundary conditions is used for the dynamic analysis of BNNT reinforced composite with attached mass. Two different cases are considered for the present study, first the effect of the varying position of attached mass on the resonant frequency of BNNT reinforced composite and second the effect of varying the value of attached mass. Mode shapes as result of analysis are shown in figures (2-7).



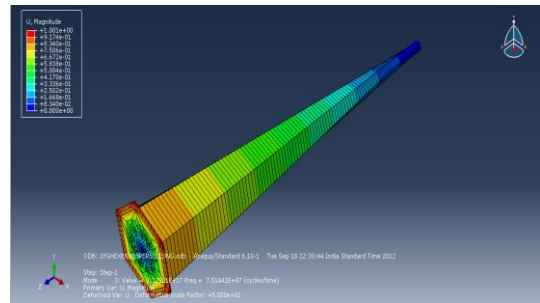
“Fig.2:Base position of BNNT composite.”



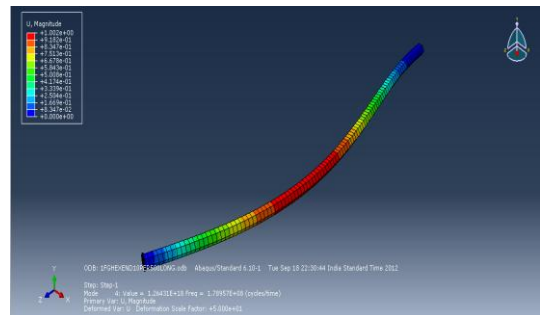
“Fig.3:First mode shape of BNNT composite.”



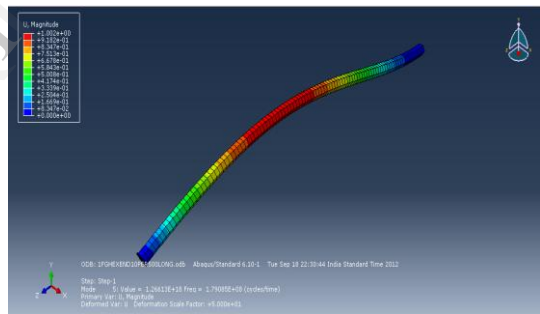
“Fig.4:Second mode shape of BNNT composite.”



“Fig.5:Third mode shape of BNNT composite.”



“Fig.6:Fourth mode shape of BNNT composite”



“Fig.7:Fifth mode shape of BNNT composite.”

The comparisons in continuum mechanics based analytical results and FEM results of the resonant frequency for different attached masses varying from $10^{-3}fg$ to $1fg$ for cantilevered configurations of SWBNNTs reinforced composite are shown in Table 2 to 5.

“Table 2: Comparison of FEM and Analytical results for $L/D=500$ and 6% volume fraction.”

Position/Mass (Kg)	One Third		Centre		End	
	FEM Solution	Analytical Solution	FEM Solution	Analytical Solution	FEM Solution	Analytical Solution
1E-21	3E+07	2.94E+07	3E+07	2.92E+07	2.9E+07	2.86E+07
1E-20	2.9E+07	2.82E+07	2.9E+07	2.68E+07	2.3E+07	2.28E+07
1E-19	2.2E+07	2.09E+07	1.9E+07	1.67E+07	1E+07	1.06E+07
1E-18	1.1E+07	8.92E+06	8268215	6.27E+06	3.51E+06	3.56E+06

“Table 3: Comparison of FEM and Analytical results for L/D=500 and 12% volume fraction.”

Position/Mass (Kg)	One Third		Centre		End	
	FEM Solution	Analytical Solution	FEM Solution	Analytical Solution	FEM Solution	Analytical Solution
1E-21	4.3E+07	4.04E+07	4.3E+07	4.01E+07	4.1E+07	3.93E+07
1E-20	4.1E+07	3.87E+07	3.9E+07	3.69E+07	3.3E+07	3.13E+07
1E-19	3.1E+07	2.87E+07	2.7E+07	2.30E+07	1.5E+07	1.46E+07
1E-18	1.5E+07	1.23E+07	1.1E+07	8.62E+06	5080220	4.90E+06

“Table 4: Comparison of FEM and Analytical results for L/D=100 and 6% volume fraction.”

Position/Mass (Kg)	One Third		Centre		End	
	FEM Solution	Analytical Solution	FEM Solution	Analytical Solution	FEM Solution	Analytical Solution
1E-21	7.51E+08	7.21E+08	7.3E+08	7.02E+08	6.85E+08	6.38E+08
1E-20	6.39E+08	6.04E+08	5.6E+08	5.15E+08	3.96E+08	3.53E+08
1E-19	3.43E+08	3.03E+08	2.8E+08	2.17E+08	1.69E+08	1.25E+08
1E-18	1.39E+08	1.04E+08	9.3E+07	7.15E+07	54106540	4.01E+07

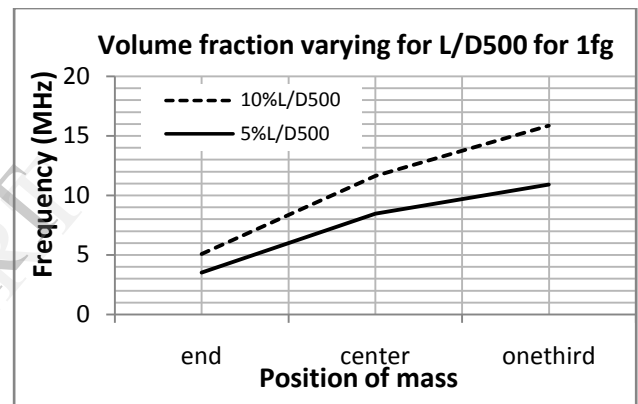
“Table 5: Comparison of FEM and Analytical results for L/D=100 and 12% volume fraction.”

Position/Mass (Kg)	One Third		Centre		End	
	FEM Solution	Analytical Solution	FEM Solution	Analytical Solution	FEM Solution	Analytical Solution
1E-21	1.01E+09	9.90E+08	994681792	9.64E+08	8.87E+08	8.77E+08
1E-20	8.63E+08	8.30E+08	729371264	7.07E+08	4.93E+08	4.84E+08
1E-19	4.56E+08	4.17E+08	320672320	2.98E+08	1.75E+08	1.72E+08
1E-18	1.71E+08	1.43E+08	115357952	9.82E+07	55898656	5.51E+07

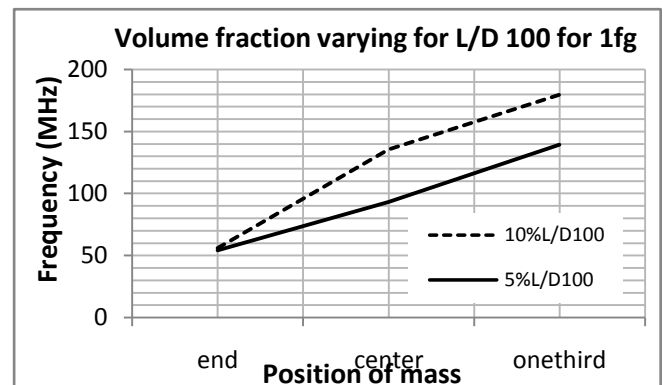
Tables 2 and 3 represent the comparative results for the resonant frequency due to different masses attached at different positions of composite for constant L/D ratio of 500 and varying volume fraction of BNNT (6% and 12%) in composite, respectively. The systematic analysis of wide range of the applications of BNNTs, e.g., nanoresonators, nanosensors, actuators and transducers, the simulation results based on FEM are compared with the continuum mechanics based

analytical approach and found in good agreement with later methodology. Similarly, the comparison of FEM and analytical results are described in Table 4 and 5 for L/D ratio of 100.

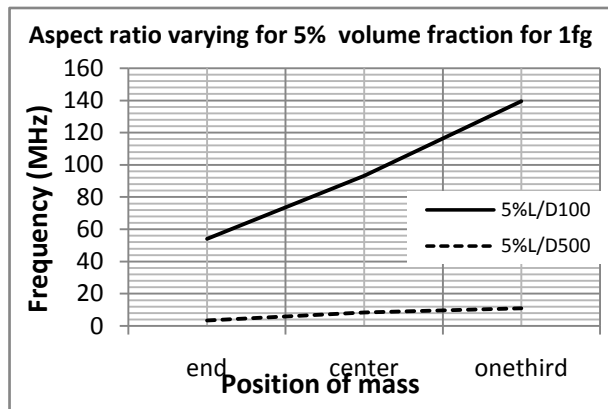
Figure 8 and 9 represents the variation in frequency due to varying volume fraction of BNNT in composite for L/D ratio of 500 and 100 with attached mass of 1.0 fg at end, centre and one-third position of composite. It is clear from the Fig. (8 and 9) that the resonance frequency increases with increase in volume fraction of BNNT in composite. This is due to fact that with increase in volume fraction there is increase in stiffness of the composite, through which the excitation rises. The reverse phenomena is observed in Fig. 10 and 11, which represents decrease in resonance frequency with increase in L/D ratio for fixed volume fraction of BNNT in composite.



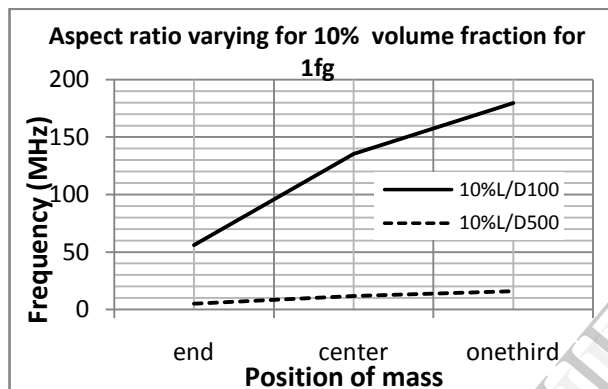
“Fig.8: Effect of volume fraction on frequency for L/D ratio of 500.”



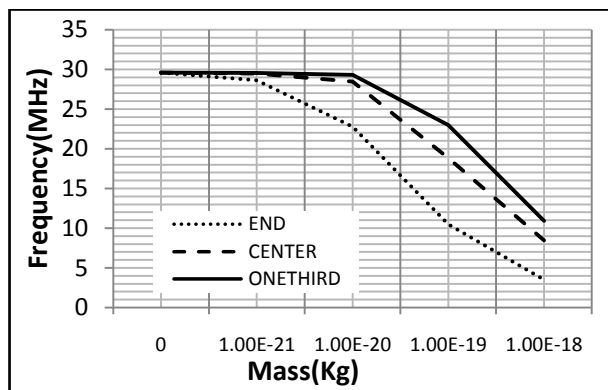
“Fig.9: Effect of volume fraction on frequency for L/D ratio of 500.”



“Fig.10: Effect of aspect ratio on frequency for volume fraction of 5%.”



“Fig.11: Effect of aspect ratio on frequency for volume fraction of 5%.”



“Fig.12: Effect of resonance frequency with varying mass attached at different position”

The variation in resonance frequency with attached mass is represented in Fig. 12 for L/D ratio of 500 with 6% volume fraction. It is clear that frequency decreases as the value of attached mass on composite increases.

Also, the effect of position of mass can be seen in Fig.12, which clearly demonstrates that as the attached mass moves toward the fixed end of composite, the resonant frequency increases.

“5. Conclusion”

The following conclusions can be drawn from the analysis as;

1. This work has analyzed the modelling of cantilevered BNNT composite using a Finite Element Model. This analysis explores the variations in resonant frequencies of BNNT composite caused by the changes in mass as well as the position of mass attached at composite. The mass sensitivity of BNNT composite mass sensor can reach 10^{-3} fg, as there is a clear frequency change but after this there is no significant change appears in the frequency.
2. It is also concluded that as the L/D ratio of composite increases, resonant frequency decreases. But there is an increase in resonance frequency with increase in volume fraction of BNNT in composite.
3. It is also evident that the resonant frequency decreases with the increase of attached mass and as the attached mass moves toward the fixed end, the resonant frequency increases.
4. The FEM simulation results and the trend are found in good agreement with present analytical method, which confirms the validity of the current FE model and indicates its suitability for use in the further investigation of the SWBNNT composite as a mass sensor.

References:

- [1]. X. Blase, A. Rubio, S. G. Louie And M. L. Cohen. Stability and band gap constancy of boron nitride nanotubes Europhys. Lett. 1994; 28(5): 335–340.
- [2]. Angel Rubio, Jennifer L, Corkill, and Marvin L Cohen. Theory of graphitic boron nitride nanotubes. Physical Review B. 1994; 49(7): 5081–5084.
- [3]. Dmitri Golberg, Yoshio Bando, Chengchun Tang, and Chunyi Zhi. Boron nitride nanotubes. Adv. Mater. 2007; 19: 2413–2432.
- [4]. Y Xiao, X H Yan, J X Cao, J W Ding, Y L Mao, and J Xiang. Specific heat and quantized thermal conductance of single-walled boron nitride nanotubes. Phys. Rev. B 2004; 69: 205415(1-5).
- [5]. P Kim, L Shi, AMajumdar, and P L McEuen. Thermal transport measurements of individual multiwalled nanotubes Phys. Rev. Lett 2001; 87(21): 215502(1-4).

- [6]. Nasreen G. Chopra and A. Zettl. Measurement of the elastic modulus of a multi-wall boron nitride nanotube. *Solid State Commun* 1998; 105(5): 297–300.
- [7]. Abhijit P. Suryavanshi, Min-Feng Yu, Jianguo Wen, Chengchun Tang, and Yoshio Bando. Elastic modulus and resonance behavior of boron nitride nanotubes *Appl. Phys. Lett* 2004; 84(14): 2527–2529.
- [8]. D Golberg, Y Bando, K Kurashima and T Sato. Synthesis and characterization of ropes made of BN multiwalled nanotubes *Scr. Mater* 2001; 44 1561–1565.
- [9]. Ying Chen, Jin Zou, Stewart J. Campbell, and Gerard Le Caer. Boron nitride nanotubes: pronounced resistance to oxidation *Appl. Phys. Lett* 2004; 84(13): 2430–2432.
- [10]. C Y Zhi, Y Bando, C C Tang, Q Huang and D Golberg. Boron nitride nanotubes: functionalization and composites, *J. Mater. Chem* 2008; 18: 3900–3908.
- [11]. Chunyi Zhi, Yoshio Bando, Chengchun Tang, Susumu Honda, Kazuhiko Sato, Hiroaki Kuwahara, and Dmitri Golberg. Characteristics of Boron Nitride Nanotube– Polyaniline Composites. *Angew. Chem. Int. Ed.* 2005; 44: 7929 –7932.
- [12]. Suman K Samanta, A Gomathi, Santanu Bhattacharya and C N R Rao. Novel Nanocomposites Made of Boron Nitride Nanotubes and a Physical Gel. *Langmuir, American Chemical Society.* 2010; 26(14): 12230–12236.
- [13]. Xuedong Bai, Dmitri Golberg, Yoshio Bando, Chunyi Zhi, Chengchun Tang, Masanori Mitome, and Keiji Kurashima. Deformation-Driven Electrical Transport of Individual Boron Nitride Nanotubes. *Nano Letters.* 2007; 7(3): 632-637.
- [14] J Wu, Wei-Qiang Han, W Walukiewicz, J W Ager, W Shan, E E Haller, and A Zettl. Raman Spectroscopy and Time-Resolved Photoluminescence of BN and B_xC_yN_z Nanotubes. *Nano Letters.* 2004; 4(4): 647-650.
- [15]. Renzhi Ma, Yoshio Bando, Hongwei Zhu, Tadao Sato, Cailu Xu, and Dehai Wu. Hydrogen Uptake in Boron Nitride Nanotubes at Room Temperature. *J. American Chemical Society.* 2002; 124: 7672-7673.
- [16]. Takeshi Terao, Chunyi Zhi, Yoshio Bando, Masanori Mitome, Chengchun Tang and Dmitri Golberg. Alignment of Boron Nitride Nanotubes in Polymeric Composite Films for Thermal Conductivity Improvement. *J. Phys. Chem. C* 2010; 114: 4340–4344
- [17]. T Thundat, P I Oden, and R J Warmack. Microcantilever Sensors. *Microscale Thermophysical Engineering.* 1997; 1: 185 – 199.
- [18]. B Ilic, D Czaplewski, H G Craighead, P Neuzil, C Campagnolo et al. Mechanical resonant immunospecific biological detector. *Appl. Phys. Lett.* 2000; 77(3): 450-452.
- [19]. Nickolay V Lavrik and Panos G Datskos. Femtogram mass detection using photothermally actuated nano mechanical resonators. *Appl. Phys. Lett.* 2003; 82(16): 2697-2699.
- [20]. M V Kireitse, G R Tomlinson, J Lu, H Altenbach, G Rongong, L V Bochkareva and D Hui. Preliminary Results on Vibration Damping Properties of Nanoscale-Reinforced Materials. *Proceeding of ENS 05 conference Paris, France, December 2005.*
- [21]. J L Arlett, E B Myers and M L Roukes. Comparative advantages of mechanical biosensors. *Nature Nanotechnology.* 2011; 6: 203-215.
- [22]. Taeyun Kwon, Kilho Eom, Jinsung Park, Dae Sung Yoon, Hong Lim Lee et al. Micromechanical observation of the kinetics of biomolecular interactions. *Applied Physics Letters.* 2008; 93: 173901(1-3).
- [23]. Gianni Ciofani, Vittoria Ruffa, Arianna Menciasia, Alfred Cuschieria. Boron nanotubes: An innovative tool for nanomedicine. *Nano Today.* 2009; 4: 8-10.
- [24]. C Y Wang, C Q Ru, and A Mioduchowski. Pressure effect on radial breathing modes of multiwall carbon nanotubes *Biochem J. Appl. Phys.* 2005; 97: 024310(1-10).
- [25]. Fabrizio Scarpa and Sondipon Adhikari. A mechanical equivalence for Poisson's ratio and thickness of C–C bonds in single wall carbon nanotubes. *J. Phys. D: Appl. Phys.* 2008; 41: 085306 (1-5).
- [26] R Chowdhury, C Y Wang and S Adhikari. Low frequency vibration of multiwall carbon nanotubes with heterogeneous boundaries. *J. Phys. D: Appl. Phys.* 2010; 43: 085405 (1-8).
- [27]. Anand Y Joshi, S P Harsha and Satish C Sharma. Vibration signature analysis of single walled carbon nanotube based nanomechanical sensors. *Physica E.* 2010; 42: 2115–2123.
- [28]. Hurang Hua, Landon Onyebueke and Ayo Abatan. Characterizing and Modeling Mechanical Properties of nano composites- Review and Evaluation, *Journal of Minerals & Materials Characterization & Engineering,* 2010; 9(4): 275-319.
- [29]. Dong Qian, Gregory J Wagner, and Wing Kam Liu, Min-Feng Yu and Rodney S Ruoff. Mechanics of carbon nanotubes. *Appl Mech Rev.* 2002; 55(6): 495-532.
- [30]. Marino Arroyo and Ted Belytschko. Continuum mechanics modelling and simulation of carbon nanotubes. *Kluwer Academic Publishers.* Printed in the Netherlands. 2005; 0:54(1-19).
- [31]. M. Arroyo and T. Belytschko. Nonlinear Mechanical Response and Rippling of Thick Multiwalled Carbon Nanotubes. *Physical Review Letters.* 2003; 91(21): 215505(1-5).

[32]. Gregory M Odegard, Thomas S Gates, Lee M Nicholson and Kristopher E Wise. Equivalent-Continuum Modeling of Nano-Structured Materials. Composites Science and Technology. 2002; 62(14): 1869-1880.

[33]. X Y Wang and X Wang. Numerical simulation for bending modulus of carbon nanotubes and some explanations for experiment. Composites: Part B. 2004; 35:79-86.

[34]. B I Yakobson, C J Brabec and J Bernholc. Nanomechanics of Carbon Tubes: Instabilities beyond Linear Response. Physical Review Letters. 1996; 76(14): 2511-2514.

IJERT